

Prediction of Multiple Binding Modes of the CDK2 Inhibitors, Anilinopyrazoles, Using the Automated Docking Programs GOLD, FlexX, and LigandFit: An Evaluation of Performance

Hideyuki Sato,^{*,†} Lisa M. Shewchuk,[‡] and Jun Tang^{†,§}

Chemistry Department, Tsukuba Research Laboratories, GlaxoSmithKline K.K., 43 Wadai, Tsukuba, Ibaraki 300-4247, Japan, and Computational, Structural and Analytical Sciences, GlaxoSmithKline Inc., Five Moore Drive, Research Triangle Park, North Carolina 27709

Received May 8, 2006

Anilinopyrazoles as CDK2 inhibitors can adopt multiple binding modes depending on the substituents at the 5-position of the pyrazole ring, based on CDK2/cyclin A crystallographic studies. Three commercially available docking programs, FlexX, GOLD, and LigandFit, were tested with 63 anilinopyrazole analogues in an attempt to reproduce the binding modes observed in the crystal structures. Each docking program gave different ligand conformations depending on the scoring or energy functions used. FlexX/drugscore, GOLD/chemscore, and LigandFit/plp were the best combinations of each docking program in reproducing the ligand conformations observed in the crystal structures. The 63 analogues were divided into two groups, type-A and type-B, depending on the substituent at the 5-position of the pyrazole ring. Although an alternate binding mode, observed in a crystal structure of one type-B compound, could not be reproduced with any of the above docking/scoring combinations, GOLD, with a template constraint based on the crystal structure coordinates, was able to reproduce the pose. As for type-A compounds, all docking conditions yielded similar poses to those observed in crystal structures. When predicting activities by scoring programs, the combination of docking with LigandFit/plp and scoring with LIGSCORE1_CFF gave the best correlation coefficient ($r = 0.60$) between experimental pIC_{50} values and top-ranked rescoring of 30 poses of each compound. With regard to type-A compounds, the correlation was 0.69. However, when 11 compounds, whose top-ranked rescored poses did not demonstrate the correct binding modes in reference to the crystal structure, were removed, the correlation rose to 0.75. Consequently, predicting activity on the basis of correct binding modes was found to be reliable.

INTRODUCTION

The number of therapeutic targets continues to grow, due to the progress in postgenomic science following completion of the human genome project. At the same time, compound collections in pharmaceutical companies are also increasing with recent progress in medicinal chemistry methods. Under these circumstances, identifying active compounds through experimental or virtual high-throughput screenings has become even more important. Therefore, further improvements in the virtual screening, facilitated by computational chemistry, are expected to dramatically speed up the drug discovery processes. However, it can still be difficult to identify active compounds with current virtual screening methods.

One of the advantages of computational chemistry is the ability to simulate experimental phenomena in virtual space. Virtual screening using computational chemistry has proven to be an effective approach in identifying active compounds from huge compound libraries. It can be classified into two

major approaches: ligand structure-based^{1–4} and protein structure-based approaches.^{5–9} The former is usually based on profiles or similarity of active compounds identified by high-throughput screenings. The profiles are calculated as descriptors defined from 2D or 3D structural information, and fingerprinting is often used for the similarity analysis. The latter usually uses docking-based screening based on interactions observed between ligands and protein in crystal structures. When target protein crystal structures are available, this approach is widely used in the drug discovery processes, as it is a more reliable and accurate method to evaluate compounds against a particular target, even though protein structure-based screening is often more time-consuming than ligand structure-based screening. Docking and scoring approaches can also be used for lead optimization as well as for virtual screening. It helps us understand the environment around ligands in the active site, allowing medicinal chemists to design and modify compounds from initial leads.

There are now 518 known human protein kinases from genome analysis (kinome¹⁰), and most of them play essential roles in signaling pathways. Because of the roles they play in the genesis of diseases such as cancer, inflammation, diabetes, cardiovascular, etc., they are important therapeutic targets. Recent activity aimed at such targets has resulted in agents such as gefinitib, used as an anticancer agent.¹¹

* Corresponding author phone: +81-29-864-6494; fax: +81-29-864-5559; e-mail: Hideyuki.Sato@gsk.com.

[†] Chemistry Department, Tsukuba Research Laboratories, GlaxoSmithKline K.K.

[‡] Computational, Structural and Analytical Sciences, GlaxoSmithKline Inc.

[§] Current address: High Throughput Chemistry, GlaxoSmithKline Inc., Five Moore Drive, Research Triangle Park, North Carolina 27709.

The cyclin-dependent kinases (CDKs) are key regulators of the cell cycle.¹² Within the CDK family, CDK2 is considered to be therapeutically important,^{13–15} since peptide inhibitors of CDK2 have been shown to induce programmed cell death (apoptosis) in transformed cells.¹⁶ It is known that the activity of CDKs is dependent upon the presence of a regulatory subunit called cyclin. Members of the cyclin family bind to and activate their CDK partners.¹⁷ CDK2 is regulated by both cyclin A and E.¹⁸ A number of small molecule inhibitors^{19–22} of CDK2 were found to show activity, including the anilino-pyrazoles. We have also reported the X-ray crystal structure of a complex of CDK2/cyclin A with an anilino-pyrazole inhibitor.²³

There have been numerous successful studies focused on predicting binding affinity using various docking and scoring programs as tools for virtual screening, and the utility of such tools has been well established.^{5,7–9,24} Kinases are attractive targets for such approaches, since a large number of kinase crystal structures have been solved complexed with a wide variety of inhibitors. The ability to accurately predict correct binding modes of active compounds, identified from high-throughput or virtual screening, will facilitate the drug discovery process. Here in, we describe the use and evaluation of a variety of docking programs and their internal scoring functions to predict the binding modes of a series of anilino-pyrazole as CDK2 inhibitors. Since the X-ray crystallographic studies indicated that this chemical series has two potential binding modes in CDK2, we will carefully discuss whether docking programs can reproduce both of the observed binding modes. Moreover, we will show that predicting activity in the context of the correct binding mode, produced by docking programs, can improve the correlation between the measured and predicted pIC_{50} s.

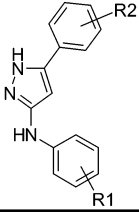
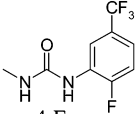
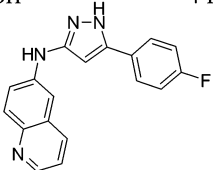
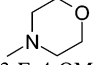
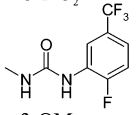
METHOD

Protein. The X-ray crystal structures of cyclin dependent kinase-2 (CDK2) complexed with cyclin A and compound **33** or **47** (Tables 1 and 2) have been solved (Figure 1²³). The structures consist of full length, nonphosphorylated CDK2 complexed with residues 173–432 of cyclin A. Although both crystal structures were only solved to low resolution (3.0 Å), the ligand orientations could be unambiguously determined due to the presence of a bromine atom in both inhibitors.

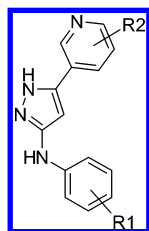
For docking calculations, the inhibitors (compound **33** or **47**), cyclin A, and all water molecules were removed from the structures. All hydrogen atoms were generated by the CHARMM²⁵ RTF method, provided as a part of QUANTA2000.²⁶ All of the acidic and basic residues in the structures were prepared as the ionic form by default. Generated hydrogen atoms were optimized by the Hydrogen Optimize method resident in QUANTA2000, which was provided as an HBUILD stream script using CHARMM. This process was repeated three times until all the hydrogen atoms were optimized. Protein structures were exported as PDB files from QUANTA2000. The structure with compound **47** was used to reproduce the alternative binding mode of compound **47** and dock type-B compounds under a template constraint method of GOLD. The crystal structure with compound **33** was used for all other calculations.

Ligands. Sixty-three inhibitors, described in Tables 1 and 2, were saved as a SMILES file, and the hydrogen position

Table 1. Compounds with a Phenyl Ring on the 5-Position of the Pyrazole Ring (Type-A)

			
Compound	pIC_{50}	R ₁	R ₂
1	5.20	4-NHCONHPh	3-Br
2	5.20	3-OBz	3-Br
3	5.23	4-NHCOMe	3-Br
4	5.32	3-OH	H
5	5.36	4-NH ₂	3-Br
6	5.36	4-SO ₂ NH ₂	4-NHCOMe
7	5.51	3,4,5-OMe	3- 
8	5.53	3,4-OMe	4-F
9	5.56	4-NO ₂	3-Br
10	5.57	3-NHCOMe	3-Br
11	5.65	3-Cl, 4-CN	4-F
12	5.65	3-OH	3-Br
13	5.67	3-OBz	4-Br
14	5.69	3-NO ₂	3-Br
15	5.73	4-NHSO ₂ Ph	3-Br
16	5.81	3-NHSO ₂ Me	3-Br
17	5.81	3-NHCOMe	H
18	5.89	3-OH	4-Br
19	5.95		
20	6.03	4-SO ₂ NH ₂	4-NHSO ₂ Ph
21	6.04	4-OH	3-Br
22	6.06	3-SO ₂ NH ₂	4-F
23	6.22	4-NHSO ₂ Me	3-Br
24	6.22	4-SO ₂ NH ₂	4-NHSO ₂ Me
25	6.31	4-SO ₂ NH ₂	3- 
26	6.39	4-SO ₂ NH ₂	3-F, 4-OMe
27	6.45	4-CONH ₂	4-F
28	6.49	4-OH	4-Br
29	6.78	4-SO ₂ NH ₂	3-NH ₂
30	6.90	4-SO ₂ NH ₂	3-NO ₂
31	7.21	4-SO ₂ NH ₂	3- 
32	7.61	4-SO ₂ NH ₂	3-OMe
33	7.63	4-SO ₂ NH ₂	3-Br
34	7.76	4-SO ₂ NH ₂	4-F
35	7.90	4-SO ₂ NH ₂	3-F, 4-OH
36	7.97	4-SO ₂ NH ₂	3-NHSO ₂ Me
37	7.97	4-SO ₂ NH ₂	3-NHSO ₂ Ph
38	8.00	4-SO ₂ NH ₂	4-Br
39	8.04	4-SO ₂ NH ₂	3-OH
40	8.11	4-SO ₂ NH ₂	4-NH ₂
41	8.76	4-SO ₂ NH ₂	3-NHCOMe
42	9.48	4-SO ₂ NH ₂	4-NO ₂

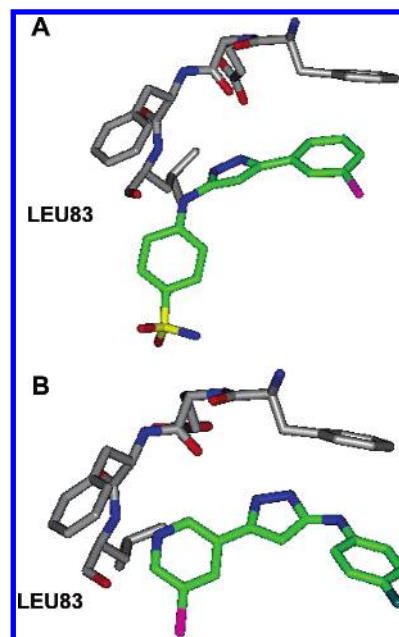
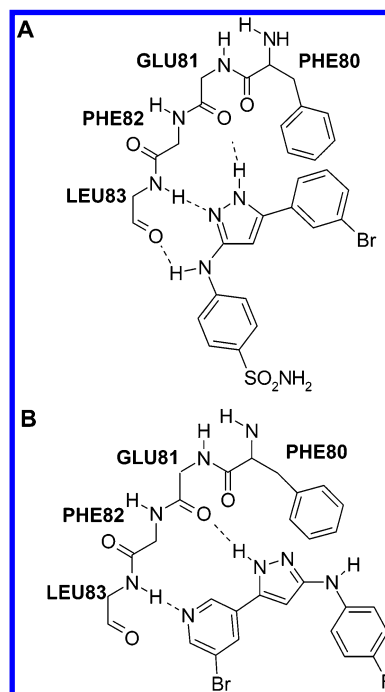
on the pyrazole ring was adjusted according to the crystal structures as described in Figure 2. Initial 3D structures for each ligand were generated from the SMILES file prepared above by CONCORD provided as a part of Sybyl 6.9.1.²⁷ The ligand structures were saved as a SD file and mol2 files.

Table 2. Compounds with a Pyridine Ring on the 5 Position of the Pyrazole Ring (Type-B)

compd	pIC ₅₀	R ₁	R ₂
43	5.35	4-NH ₂	3-Br
44	5.36	4-NHCOMe	3-Br
45	5.38	4-NHCOCH ₂ OMe	3-Br
46	5.42	4-NHCOPh	3-Br
47	5.51	4-F	3-Br
48	5.54	4-CF ₃	3-Br
49	5.62	3-NH ₂	3-Br
50	5.67	3-OBz	3-Br
51	5.68	3-NHCOPh	3-Br
52	5.86	3-NHCOMe	3-Br
53	5.86	4-OH	3-Br
54	5.89	4-NHSO ₂ Ph	3-Br
55	5.94	3-SO ₂ NH ₂	3-Br
56	5.98	3-NHSO ₂ Ph	3-Br
57	6.04	3-OH	3-Br
58	6.26	3-NHSO ₂ Me	3-Br
59	6.28	4-NO ₂	3-Br
60	6.49	3-F	3-Br
61	6.76	3-NO ₂	3-Br
62	6.76	4-SO ₂ NH ₂	H
63	6.79	4-SO ₂ NH ₂	3-Br

Docking Programs. *FlexX*. *FlexX*,^{28–30} which is a part of Sybyl 6.9.1, was used in our comparison studies. *FlexX* gives the best poses at the binding site by an incremental algorithm with flexible conformations. The binding site for calculations was defined with default parameters as all atoms of CDK2 within 10 Å of LEU134. The defined site completely covered the known ATP binding site of CDK2. The formal charge of each compound was assigned during the calculations by *FlexX*, and 30 poses for each compound were generated. Either scoring function of *flexxscore* or *drugscore* was selected for each condition. Other parameters were not changed from the default. Results were saved in Sybyl database format. The poses, saved as a mol2 files per each condition, were converted into SD files with all hydrogen atoms.

GOLD. A standard mode of GOLD 2.1.1^{31–34} was used in our comparison studies. GOLD gives the best poses by a genetic algorithm (GA) search strategy, and then various molecular features are encoded as a chromosome. A binding site was defined as all atoms of CDK2 within 10 Å of the C γ atom of LEU134. The defined binding site is essentially the same as the site used with *FlexX*. The default calculation mode, which provides the most accurate docking results, was selected for all calculations. In the standard calculation mode, by default, the GA run comprised 100 000 genetic operations on an initial population of 100 members divided into five subpopulations, and the annealing parameters of fitness function were set at 4.0 for van der Waals and 2.5 for hydrogen bonding. Default parameters were also selected for others. The number of generated poses was set to 30, and early termination was turned off. Each compound was imported from a mol2 file, and the generated poses were

**Figure 1.** Crystal structures of compounds 33 (A) and 47 (B) in CDK2/cyclin A. Carbon atoms of CDK2 were shown in gray, and carbons of the ligands were shown in green. Compound 33 made a hydrogen bond between its pyrazole N and the HN of LEU83, while compound 47 made a hydrogen bond to the NH of LEU83 via its pyridine N. Resolutions of both crystal structures were 3.0 Å.**Figure 2.** (A) Hydrogen bonding predicted from the crystal structure of compound 33. Three point hydrogen bonds were expected. (B) Hydrogen bonding predicted from the crystal structure of compound 47. Two hydrogen bonds were expected.

exported as mol2 files. Atom types for ligands and the protein were set during the calculation by GOLD. The scoring function of either *goldscore* or *chemscore* was selected for each condition.

A template constraint, based on the crystal structure of compound 47, was used in reproducing the binding mode observed in the crystal structure. The constraint was applied with 1000 spring values, and the same parameters were used

above. CDK2 coordinates from the crystal structure of compound **47** were used for this calculation. As in the nonconstraint docking studies, the binding site was defined as all atoms of the CDK2 within 10 Å of the C γ of LEU134. The Scoring function of either goldscore or chemscore was selected for each condition, as deemed appropriate.

LigandFit. LigandFit,³⁵ which is a part of Cerius2 4.8.1,²⁶ was used in all calculations. LigandFit gives the best poses at the binding site by a stochastic conformational search and the energy of the ligand–protein complex. It uses a grid method when evaluating interactions between the protein and the ligand. The binding site for the calculations can be defined by either the flood filling method, which is a cavity search algorithm based on protein shape or the ligand coordinates in a model or from experimental data, such as a crystal structure. In our case, the flood filling method did not find the ATP binding site. The site defined by the method was too small to cover either ATP binding site or the ligand binding site observed in the crystal structures. Enlarging the site was required to cover the binding site. However, calculations with this enlarged site yielded no poses similar to the crystal structure. Therefore, the active site was generated from the ligand coordinates in the crystal structure of CDK2/cyclin A complexed with compound **33** using default parameters. The defined active site size was much smaller than the one defined for FlexX and GOLD. The energy of the grid was set using PLP^{36,37} or DREIDING³⁸ or CFF.³⁹ Thirty poses were generated by each condition with default parameters. The SD file was used as an input file of the ligands.

Scoring Programs. **CSCORE.** CSCORE, which is provided as a part of Sybyl 6.9.1, was used. CSCORE provides D_SCORE,^{40,41} CHEMSCORE,⁴² PMF_SCORE,⁴³ and G_SCORE^{32,34} to describe affinities of poses against a protein. D_SCORE is based on both electrostatic and hydrophobic contributions for binding but does not include entropic terms. CHEMSCORE is dependent on lipophilic interactions, hydrogen bonding, and loss of ligand flexibility based on a training set of 82 ligand–protein complexes. PMF_SCORE relies on ligand–protein and atom-pair interactions from crystal structures in the PDB. Finally, G_SCORE uses hydrogen-bonding interactions that incorporate desolvation of donors and acceptors. Poses, saved as SD files, and the protein structure, used for the docking calculations, were imported into Sybyl for the CSCORE calculations. Scores of all poses were calculated vs the protein structure used for docking calculations above.

LigScore. LigScore is a part of Cerius2 4.8.1. LigScore provides LIGSCORE1_DREIDING, LIGSCORE1_CFF, LIGSCORE2_DREIDING, LIGSCORE2_CFF,⁴⁴ PLP1,³⁶ PLP2,³⁷ PMF,⁴³ and JAIN.⁴⁵ LIGSCORE is based on three descriptors; vdW, c+pol, and Totpol2. The vdW is a Lennard-Jones 6–9 potential on a grid. The c+pol is a count of the buried polar surface area between a ligand and a protein involving attractive ligand–protein interaction. The Totpol2 is a count of the buried polar surface area between a ligand and a protein involving both attractive and repulsive ligand–protein interactions. LIGSCORE uses DREIDING and CFF force field parameters for grid based and exact pairwise calculations of vdW. PMF is based on a statistical analysis in crystal structures and defined as the sum of the interaction free energies over all interatomic pairs of ligand–

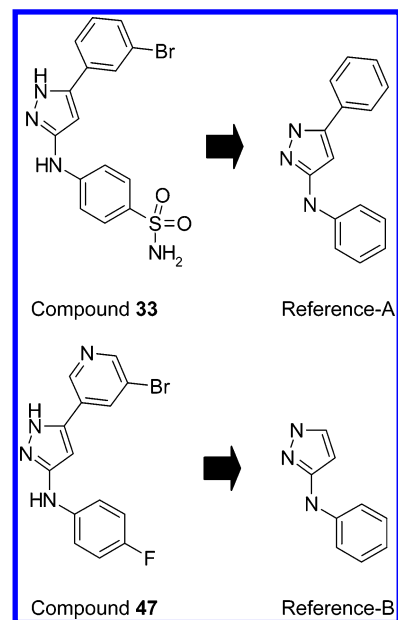


Figure 3. Reference-A, whose corresponding coordinates were derived from the crystal structure of compound **33**, was used to calculate RMSD values of type-A compounds. Reference-B, whose corresponding coordinates were derived from the crystal structures of compound **33** or **47**, was used to calculate RMSD values of type-B compounds.

protein complex. PLP is piecewise linear potential. A grid for LigScore calculations was defined to cover all the poses by expanding the grid used for LigandFit calculations. Poses, saved as SD files, and the protein structure, used for the docking calculations, were imported into Cerius2. Scores of all poses saved as SD files from the above docking calculations were calculated against the protein structures used for the docking calculations above.

RMSD Calculation. In calculating RMSD values of all poses against the crystal structures of compound **33** or **47** by using an SPL program provided by Dr. Toshiro Kimura (Sumisho Computer Systems, Japan) in Sybyl 6.9.1, two reference structures were defined as described in Figure 3. Reference-A was used to calculate RMSD values of type-A compounds against the crystal structure of compound **33**. Its coordinates were derived from the crystal structure. Reference-B was used to calculate RMSD values of type-B compounds against the X-ray structure of compound **47**. Its coordinates were derived from the crystal structure. In the reference structures, all hydrogen atoms were removed. RMSD values were calculated only for corresponding atoms between the reference and pose.

Computer Environment. All docking and scoring calculations were done on a Silicon Graphics Fuel with a single processor of R14000 600 MHz and RAM of 1GB. Protein structures were compiled in QUANTA2000, and all docking results were visualized in Sybyl 6.9.1. Both visualizations were done on the visual workstation.

RESULTS AND DISCUSSION

Sixty-three anilinopyrazole analogues, with a wide range of potencies against CDK2/cyclin A, were described in Tables 1 and 2. The compounds are divided into two groups (type A and B) based on the substituents at the 5-position of the pyrazole ring, since we observed that this series of

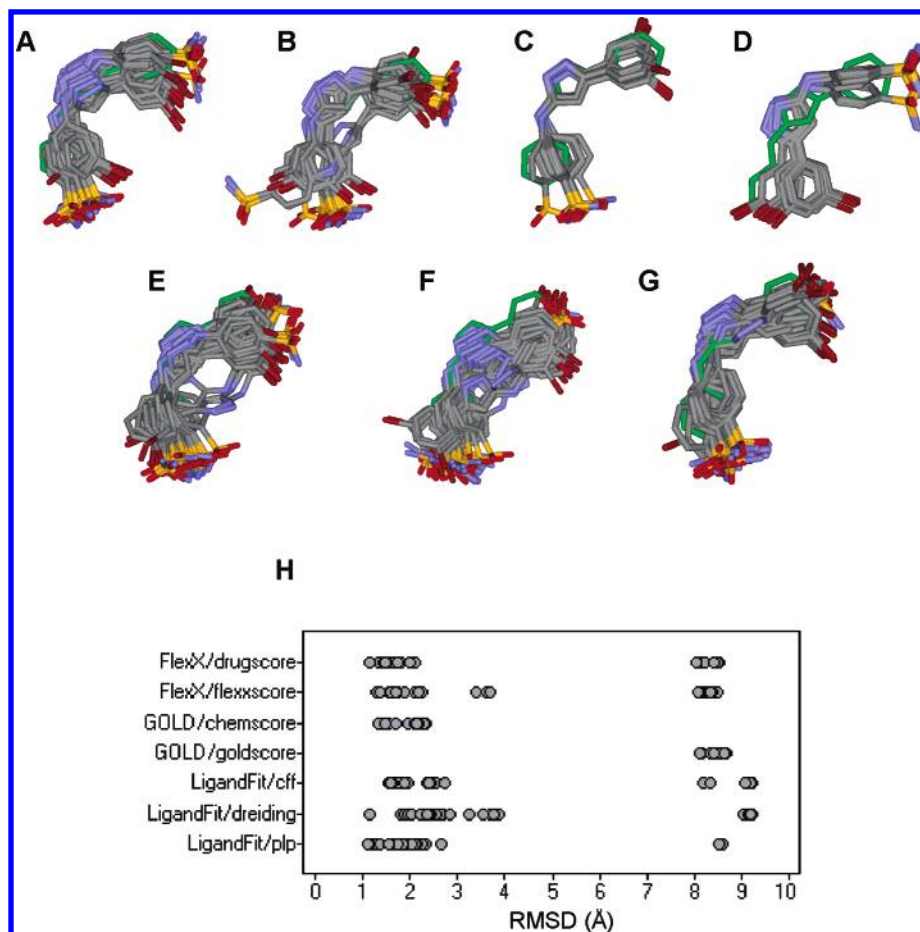


Figure 4. Results of docking poses of compound **33**. Thirty poses produced by seven docking conditions were overlaid with a reference structure (green) in the crystal structure. **A**: FlexX/drugscore, **B**: FlexX/flexscore, **C**: GOLD/chemscore, **D**: GOLD/goldscore, **E**: LigandFit/cff, **F**: LigandFit/dreiding, **G**: LigandFit/plp. RMSD values of each pose against the reference were plotted in **H**.

compounds had at least two binding modes, as shown in Figure 1.

Crystal Structure of Compound 33 and Reproducing the Crystal Structure by Docking Programs. The crystal structure of compound **33**, a representative type-A compound, complexed with CDK2/cyclin A (Figure 1A) was solved. In the structure, three hydrogen bonds were observed between the compound and CDK2/cyclin A as described in Figure 2A. The p-sulfonamidobenzyl group was located at the solvent front, near HIS84 and ASP86. The 3-bromophenyl substituent at the 5-position was close to PHE80, which is often referred to as the gatekeeper.

Since predicting the correct binding mode of each compound using docking programs is a key step if structure-based design is to be used in improving potency, three docking programs were carefully evaluated in order to investigate whether any docking programs can reproduce the inhibitor conformation observed in the crystal structure. Since the docking programs evaluated here have several scoring functions or energy calculation algorithms on grids, seven combinations were explored: FlexX/flexscore, FlexX/drugscore, GOLD/goldscore, GOLD/chemscore, LigandFit/dreiding, LigandFit/cff, and LigandFit/plp.

Poses determined by FlexX or LigandFit could be divided into two major binding modes, as shown in Figure 4A,B,E–H. One binding mode had a similar conformation to one observed in the crystal structure, while the other mode had

a flipped conformation relative to the crystal structure. On the other hand, poses determined by GOLD (Figure 4C,D,H) showed very different results from the others.

In LigandFit, combinations with three different energy functions, dreiding, cff and plp, produced different results, as shown in Figure 4E–H. Although the binding site for LigandFit was tightly defined based upon the ligand coordinates, the poses showed various locations and configurations. Poses by LigandFit/dreiding had a broad distribution and most were far from the ligand position observed in the crystal structure. Poses by LigandFit/cff were better than LigandFit/dreiding; however, 3 of the 30 poses completely missed the correct binding site for the pyrazole ring. Finally, all poses generated by LigandFit/plp placed the pyrazole ring near LEU83. However, two poses were flipped relative to the crystal structure. Therefore, LigandFit/plp gave better results to reproduce the crystal structure than those by two other LigandFit calculations.

In FlexX study, FlexX/drugscore (Figure 4A) and FlexX/flexscore calculations (Figure 4B) produced 21 and 13 poses, respectively, whose RMSDs were less than 3 Å vs the crystal structure, although both conditions used a larger binding site than that in the LigandFit study. In the FlexX/drugscore calculations, those poses that did not reproduce the conformation observed in the crystal structures showed flipped binding modes. Meanwhile, FlexX/flexscore produced 3 poses that completely missed the hinge interaction

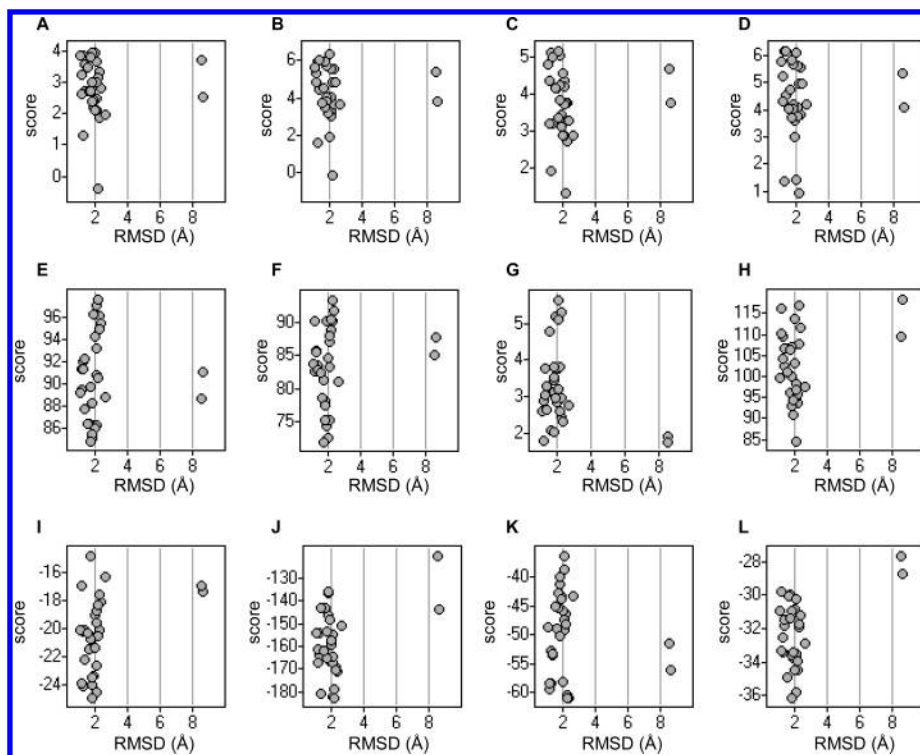


Figure 5. Correlation between scores and RMSD of poses by LigandFit/plp in reproducing the conformation of compound **33** observed in the crystal structure. CHEM_SCORE could differentiate 28 correct binding of the poses against incorrect poses; however, the correlation between score and RMSD were not linear. **A:** LigScore1_Dreiding (LigScore), **B:** LigScore1_CFF (LigScore), **C:** LigScore2_Dreiding (LigScore), **D:** LigScore2_CFF (LigScore), **E:** PLP1 (LigScore, reversed scale on Y axis), **F:** PLP2 (LigScore, reversed scale on Y axis), **G:** PMF (LigScore, reversed scale on Y axis), **H:** JAIN (LigScore, reversed scale on Y axis), **I:** F_SCORE (CSCORE), **J:** G_SCORE (CSCORE), **K:** PMF_SCORE (CSCORE), **L:** CHEM_SCORE (CSCORE).

(LEU83). Therefore, FlexX/drugscore seemed to give a better result than FlexX/flexxscore in reproducing the conformation of compound **33**.

Interestingly, GOLD showed different results from the other docking programs. GOLD/goldscore produced only poses that had flipped binding modes (Figure 4D), while GOLD/chemscore produced only poses that had correct binding modes within RMSD of 2.5 Å (Figure 4C). The RMSD differences seemed to be dependent upon the conformation of the two phenyl rings, since the pyrazole rings in the poses generated by GOLD/chemscore had essentially the same location. Although all the poses determined by GOLD/chemscore had the correct binding mode, the lowest RMSDs were higher than the ones observed with FlexX/drugscore, FlexX/flexxscore, LigandFit/dreiding, and LigandFit/plp (Figure 4H). Based on these results, we concluded that GOLD/chemscore would be a useful method to predict appropriate binding modes in our case.

As describe above, each docking condition produced different poses even with the same ligand and protein, and the quality of the docking programs was evaluated based on the accuracy of the poses as measured by the RMSD vs the ligand coordinates observed in the crystal structure. If a crystal structure was not available, we would need to evaluate the poses using other methods. Here, we utilized the scoring functions. In Figure 5, scores and RMSDs of poses by LigandFit/plp of compound **33** were plotted. It appeared that CHEM_SCORE of CSCORE gave higher values for incorrect poses than for correct ones. Consequently, although the scores might be helpful to evaluate poses, it would not be

workable, if crystal structures were not available, because there is no way to evaluate scoring itself without references.

Crystal Structure of Compound 47 and Reproducing the Crystal Structure by Docking Programs. Surprisingly, an alternate binding mode was revealed in the crystal structure of compound **47**, a representative type-B compound, complexed with CDK2/cyclin A (Figure 1B). In the structure, only two hydrogen bonds were observed between the compound and CDK2/cyclin A as described in Figure 2B. This compound, which had a pyridine ring at the 5-position, formed a hydrogen bond with the main chain NH of LEU83 using the nitrogen on the pyridine ring rather than a pyrazole nitrogen. The 4-fluoroanilino group was located near LYS33, which formed a conserved salt bridge with a glutamate in the back of the ATP binding site. The pyrazole ring was located near PHE80, the gatekeeper, and formed a hydrogen bond with GLU81, rather than interacting with the hinge region, as observed in the crystal structure of compound **33**. Therefore, we determined whether docking programs could reproduce this alternate binding mode which had two hydrogen bonds between the compound and CDK2. When the default docking conditions, used for compound **33**, were applied in reproducing compound **47**, none of the docking programs could reproduce the crystallographically observed binding mode. Instead, they all produced similar poses to what were observed for compound **33** (data not shown). To reproduce the two points binding mode, a template constraint method of GOLD was applied. With this method, the constraint is generally based on all or a part of ligand coordinates from the crystal structure or docking model. In

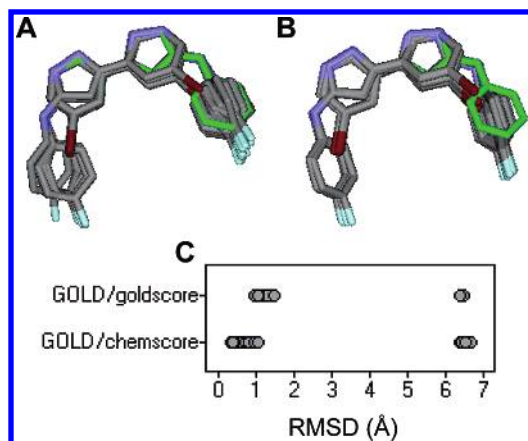


Figure 6. Results of docking poses of compound **47** by GOLD/chemscore and GOLD/goldscore with a template constraint in reference to the crystal structure of the compound. Thirty poses by each docking conditions were overlaid with a reference structure (green) in the crystal structure. **A:** GOLD/chemscore, **B:** GOLD/goldscore. RMSD values of each pose against the reference were plotted in **C**.

this study, the template was defined by the coordinates of compound **47** in the crystal structure, but the fluorine and chlorine atoms were removed from the coordinates. GOLD required 1000 spring value as a template constraint for the calculations which used the same condition to what was used in reproducing compound **33** except for the constraint. Two scoring functions of GOLD were similarly compared. Both conditions produced poses which had two hydrogen bonds between the compound and the protein as observed in the crystal structure (Figure 6). GOLD/chemscore produced more correct poses than GOLD/goldscore. Therefore, it seemed that GOLD/goldscore and GOLD/chemscore without any constraints were not appropriate in reproducing the binding mode; however, GOLD with the template constraint could be one of the solutions to reproduce uncommon binding modes, when complex structures were available. However, 1000 spring value is much larger than the value commonly used.

These results suggested that the docking programs, without constraint, could not reproduce the two point binding mode as a more favorable conformation than three point binding mode. Docking programs may not be able to reproduce the alternate binding mode due to the close contact between the pyrazole ring and the gatekeeper (Figure 1B). Very strong constraints were required to reproduce the binding mode. The close contact should be one of the key reasons why GOLD could not reproduce the binding mode. If the two point interaction was the main reason for the failures, such strong constraint would not be required to reproduce it.

Docking of Analogues. All analogues of anilino-pyrazoles in Tables 1 (type-A) and 2 (type-B) were docked by the seven docking conditions which were used to reproduce the crystal structure of compound **33**. As discussed in the previous section, the compound series has at least two binding modes in CDK2/cyclin A depending upon substituents at the 5-position of the pyrazole ring. However, it would be difficult to predict which binding mode was favored for each compound, because the combination of substituents should give more complicated results. Therefore, docking conditions without constraints were used for the analogues. RMSD

values of all the poses determined by seven docking conditions were calculated against the reference-A or -B in Figure 3 and plotted in Figure 7. These plots showed that most of the poses determined by all the docking conditions were given either the binding mode observed in the crystal structure of compound **33** or a flipped binding mode as described in Figure 4. In Figure 7, one group around 1 Å (group-1) consisted of poses which had the correct binding mode and desired hydrogen bonds with the hinge region of CDK2. Binding modes of the poses were similar to one observed in the crystal structure of compound **33**. The other major group around 7 Å (group-2) consisted of poses which had a flipped binding mode compared to that observed in the crystal structure with compound **33** as observed in reproducing the crystal structures in Figure 4. Other poses which did not belong to either group-1 or -2 mostly did not have hydrogen bonds with the hinge region. There was a small difference in group-2 between type-A and type-B compounds. RMSDs of type-B compounds were smaller than the ones of type-A compounds. As described in the above Method section, it was caused by the difference between reference-A and -B in calculating RMSDs. RMSDs of type-B compounds did not include conformational differences of the pyridine ring. Most poses from FlexX/drugscore, FlexX/flexxscore, GOLD/chemscore, GOLD/goldscore, and Ligand-Fit/plp belonged to two major groups, group-1 and -2, and their distributions were sharp. In particular, GOLD produced very sharp distributions by both goldscore and chemscore. However, LigandFit/cff and LigandFit/dreiding provided a broader distribution than others, although these conditions used smaller space for the docking calculations than FlexX and GOLD. In both cases, poses for type-B were also widely spread. In LigandFit/dreiding, two major groups did not clearly exist, and their ranges were much broader. On the contrary, LigandFit/plp gave a sharper distribution than LigandFit/cff or LigandFit/dreiding, but the distribution of LigandFit/plp was still broader than with FlexX and GOLD. In FlexX, FlexX/flexxscore (Figure 7B) had more poses in group-1 than FlexX/drugscore (Figure 7A); in particular, there were 4 compounds which had all poses within RMSD of 2 Å. From these results, it was expected that flexxscore was a better scoring function than drugscore for FlexX in our case.

The difference between scoring functions of GOLD was more explicit. Of type-A compounds, all poses of 19 compounds and no poses of 6 compounds were determined within RMSD of 2 Å by GOLD/chemscore. Meanwhile, all poses of 5 compounds and no poses of 19 compounds were determined within RMSD of 2 Å by GOLD/goldscore. Of 23 compounds whose activities were greater than pIC_{50} of 6, GOLD/chemscore had 16 compounds which had all poses within 2 Å and 4 compounds which had no poses within RMSD of 2 Å; meanwhile, GOLD/goldscore had 2 and 16 compounds, respectively. The results from GOLD/chemscore and GOLD/goldscore could suggest that the scoring functions in GOLD were more important to find the correct binding modes of our compound series than the other two docking programs. In fact, chemscore gave more correct poses than goldscore, and it was more explicit in the most potent compounds. Of type-B compounds, RMSD-related evaluation was more difficult, because it was expected that at least one of the anilino-pyrazoles had a different binding mode from

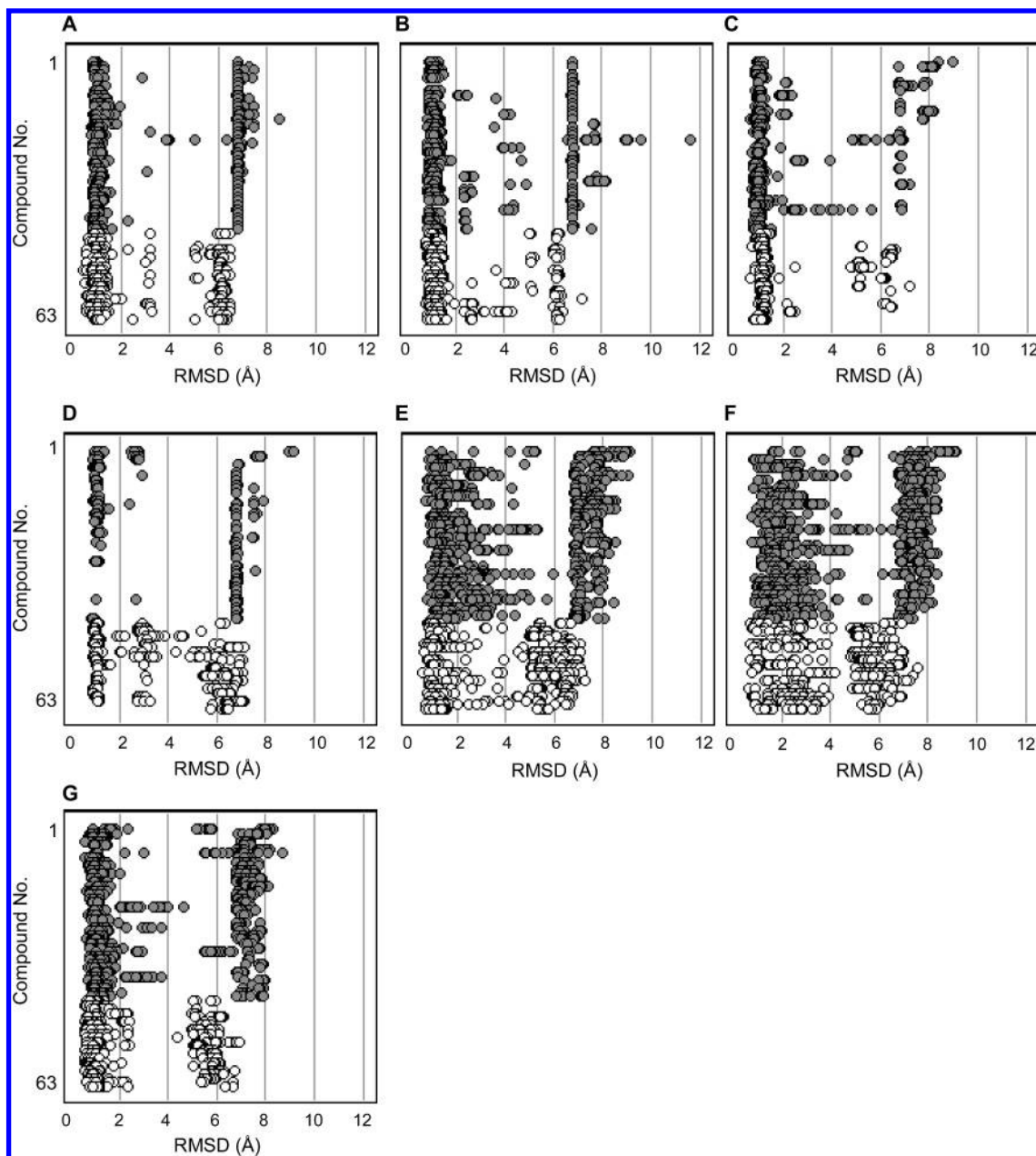


Figure 7. RMSD values of each poses of all compounds were calculated against a reference structure. Gray circles were type-A compounds, and white circles were type-B. **A:** FlexX/drugscore, **B:** FlexX/flexxscore, **C:** GOLD/chemscore, **D:** GOLD/goldscore, **E:** LigandFit/cff, **F:** LigandFit/dreiding, **G:** LigandFit/plp.

one observed in the crystal structure of compound **33**. Because all the used docking programs could not provide the binding mode of compound **47**, it seemed to be difficult to find the correct binding modes of type-B compounds. However, as expected from the results of type-A compounds, both type-A and -B compound series would basically prefer the binding mode observed in the crystal structure of compound **33** in all the docking calculations. In fact, any docking programs could not find the binding mode of compound **47** without a template constraint which was based on the crystal structure.

Consequently, it was shown that FlexX/flexxscore, GOLD/chemscore, and LigandFit/plp could determine correct binding modes, which were similar to one in the crystal structure of compound **33**, of type-A compounds; on the other hand, no docking conditions could determine correct binding modes, which were similar to one in the crystal structure of

compound **47**, of type-B compounds. It was still unclear whether all type-B compounds bind to the protein on the binding mode observed in compound **47**, because no docking conditions could show the binding mode. Results from GOLD with the template constraint, which was used to reproduce the binding mode observed in the crystal structure of compound **47**, were shown in Figure 8. In the plots, RMSD values were calculated against the reference structure in Figure 3, and most poses could be divided into two common binding modes. One binding mode was similar to one in the crystal structure of compound **47** (group-3 around 1–2 Å), and another one was similar to that of compound **33** (group-4 around 6–7 Å). GOLD/chemscore determined more poses in group-3 than GOLD/goldscore. However, there were a lot of poses which belonged to group-4, although a very strong template constraint was also used in the conditions. The result was similar to one in reproducing the crystal

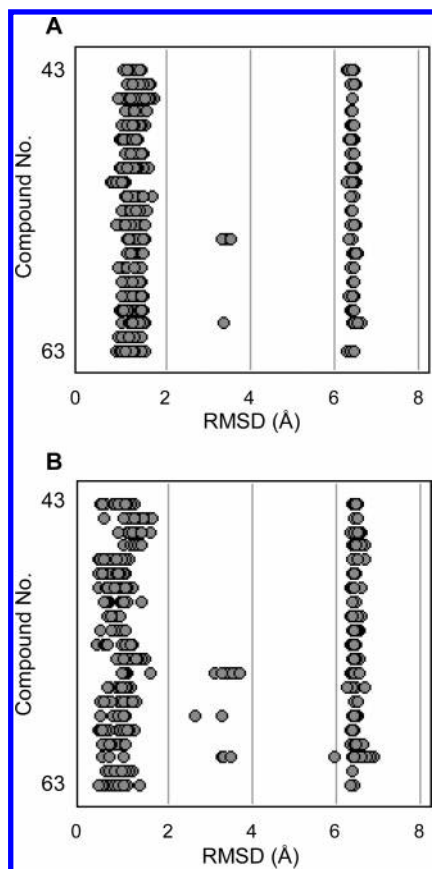


Figure 8. RMSD values of type-B compounds against a reference structure were plotted. **A** is GOLD/goldscore, and **B** is GOLD/chemscore with a template constraint of GOLD in reference to the crystal structure of compound 47.

structure of compound 47 by GOLD/chemscore and GOLD/goldscore with the template constraint in Figure 6.

Predicting Activities. Predicting the activity of a compound is the most important part of virtual screening by docking programs. If we could accurately predict potencies, it would be possible to reduce experimental efforts, and it would be necessary to confirm the activities of only a few selected compounds. However, such efforts should be discussed on the basis of having identified the correct binding modes. If the predicted activities are not based on correct binding modes, it would be difficult to correctly modify compounds from the docking models. In this section, we discuss the relationships between binding modes and predicting activities on our kinase target. Rescoring by CSCORE and LigScore was applied against all poses from all docking conditions. Correlation coefficients between the top-ranked rescored poses and activities were calculated as an r value. In most cases, a poor correlation between activity as pIC_{50} and the top-ranked rescored poses existed.

In the case of a combination of docking by LigandFit/plp and scoring by LIGSCORE1_CFF, the correlation coefficient between pIC_{50} and the top-ranked score of each compound was $r = 0.60$; however, when type-B compounds were removed from the compound set, the value increased to $r = 0.69$ (Figure 9). This improvement in correlation may be due to the complicated binding mode of type-B compounds, as the binding mode of type-B compounds has not been established by either crystal structure or docking study discussed above. Focusing on RMSD of the poses, the top-

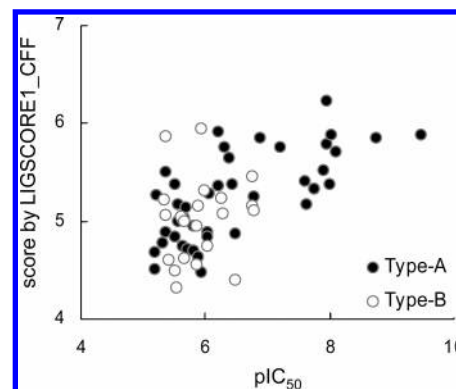


Figure 9. A plot of pIC_{50} values vs top-ranked scores by LIGSCORE1_CFF of poses by LigandFit/plp.

ranked rescored poses of 46 compounds belong to group-1, of which RMSDs were around 1.0 Å. Thirty-one of 42 type-A and 15 of 21 type-B compounds were in the group. Because 11 type-A compounds, of which the top-ranked rescored poses did not belong to group-1, were not correctly docked by LigandFit/plp, these compounds were removed from the set to confirm the relationship between the measured pIC_{50} and the score value for the correct binding modes. As a result, the correlation coefficient of 31 compounds was $r = 0.75$. On the other hand, because the correlation coefficient of 15 type-B compounds in group-1 was $r = 0.08$, it is still unclear whether the most favorable binding mode of type-B compounds is like Figure 1A,B or others. Consequently, it was demonstrated that scoring by LIGSCORE1_CFF against poses docked by LigandFit/plp could give reasonable activity prediction ($r = 0.75$).

CONCLUSIONS

Docking-based structural design is an effective method when the target structures are available; however, it is still a challenging area in drug discovery. We believe detailed discussions and understanding of the basis of binding modes would be useful in discovering or designing new potent compounds and thus could speed up the drug discovery process. It is worth comparing docking approaches used on each target, since it is still unclear which docking program is the best one, even for protein kinases, although 3D structures of protein kinases are better understood than those of other protein targets.

We found that the crystal structure of compound 33, a representative type-A compound, in CDK2/cyclin A had three hydrogen bonds between the ligand and the hinge region of the protein. These hydrogen bonds were correctly reproduced by docking programs. However, we have shown that scoring functions of docking programs were sometimes very effective in reproducing the ligand conformation. In particular, two docking conditions of GOLD gave quite different distributions of poses for compound 33. Interestingly, all the poses from GOLD/chemscore had correct poses which were close to the binding mode observed in the crystal structure; however, GOLD/goldscore yielded no correct poses. This result demonstrated that comparing docking conditions was a very important step for this target before starting the calculations against large compound sets. We have also shown that, if a crystal structure of the target with ligand was not available, it was difficult to evaluate whether

poses had the correct binding mode or not, because scoring programs could not correctly evaluate binding modes.

The crystal structure of compound **47**, a representative type-B compound, showed the alternative binding mode in CDK2/cyclin A. In the structure, only two hydrogen bonds between the ligand and the protein were observed, and the hinge region had a hydrogen bond with pyridine of the ligand. In general, we have to be careful when using binding modes observed in low resolution crystal structures. However, we have a confidence in the ligand orientation observed in the crystal structure of compound **47** due to the presence of a bromine atom. Because docking programs could not reproduce the alternative binding mode, two point interaction, without a template constraint which relied on the crystal structure, it could demonstrate that the binding mode of type-B compounds was more complicated than what we could expect from the experimental evidences.

When type-A compounds were docked, docking programs could find correct poses. However, no docking programs found the alternative binding mode of type-B compounds. LigandFit/cff or LigandFit/dreiding gave a wide range RMSD values; however, in LigandFit/plp, it was much sharper even by using the same docking program. In both FlexX conditions, it was shown that FlexX could not come under the influence of internal scoring functions strongly; therefore, these scoring functions were similar at least in our case. On the other hand, in GOLD, although the RMSD values were as sharp as in FlexX, both GOLD/goldscore and GOLD/chemscore demonstrated different characters. In particular, chemscore gave results which were similar to the ligand conformation observed in the crystal structure. This result emphasized the importance of evaluating docking conditions for targets.

Unfortunately, the correlation coefficient between the top-ranked score and measured pIC₅₀ activity was $r = 0.60$ even in the best case of LigandFit/plp and LIGSCORE1_CFF. However, when type-B compounds were removed from the compound set, the correlation increased to 0.69, and when poorly docked type-A compounds were removed from the type-A compound set, it finally increased to 0.75. If crystal structures were not available for the prediction, we could not determine such a good correlation between the measured and predicted pIC₅₀s. For type-B compounds, additional crystal structures may be required to confirm whether the alternative binding mode is commonly observed in CDK2/cyclin A.

When high resolution crystal structures are available, prediction of binding affinity should be reliable. However, if such structures are not available, it may not be possible to accurately predict them. In our case, since the resolution of both complex crystal structures was low, we need to interpret the predictions carefully. Although we have strong confidence in the ligand locations, observed in the crystal structure described above, the structures may have distortion in the vicinity of the active site, leading to difficulties in accurately predicting affinities by virtual screening. Moreover, even if high-resolution structures were available, we would have to consider issues of flexibility or solvation of the protein structure and compatibility of force field in docking and scoring programs. In drug discovery, it is often difficult to obtain high-resolution crystal structures for predicting binding affinity by virtual screening. Therefore, it is useful to

compare docking and scoring programs with representative crystal structures as reported in this article.

ACKNOWLEDGMENT

We thank Dr. Joseph H. Chan of GlaxoSmithKline, Research Triangle Park, NC, and Drs. Gregory L. Warren and Martha S. Head of GlaxoSmithKline, Upper Merion, PA, U.S.A., for their advice and proofreading for completion of this scientific article. We are also grateful to Drs. Stephen V. Frye, Drake S. Eggleston, Karen E. Lackey, and Lee F. Kuyper of GlaxoSmithKline, Research Triangle Park, NC, U.S.A., for their support to this research. We also acknowledge the technical support of Accelrys, CCDC, and Tripos for all calculations, especially Dr. Toshiro Kimura of Sumisho Computer Systems in Japan for developing SPL programs.

REFERENCES AND NOTES

- (1) Wilton, D. J.; Harrison, R. F.; Willett, P.; Delaney, J.; Lawson, K.; Mullier, G. Virtual screening using binary kernel discrimination: analysis of pesticide data. *J. Chem. Inf. Model.* **2006**, *46*, 471–477.
- (2) Hert, J.; Willett, P.; Wilton, D. J.; Acklin, P.; Azzaoui, K.; Jacoby, E.; Schuffenhauer, A. New methods for ligand-based virtual screening: use of data fusion and machine learning to enhance the effectiveness of similarity searching. *J. Chem. Inf. Model.* **2006**, *46*, 462–470.
- (3) Stahura, F. L.; Bajorath, J. New methodologies for ligand-based virtual screening. *Curr. Pharm. Des.* **2005**, *11*, 1189–1202.
- (4) Deanda, F.; Stewart, E. L. Application of the PharmPrint methodology to two protein kinases. *J. Chem. Inf. Comput. Sci.* **2004**, *44*, 1803–1809.
- (5) Kairys, V.; Fernandes, M. X.; Gilson, M. K. Screening drug-like compounds by docking to homology models: a systematic study. *J. Chem. Inf. Model.* **2006**, *46*, 365–379.
- (6) Maiorov, V.; Sheridan, R. P. Enhanced virtual screening by combined use of two docking methods: getting the most on a limited budget. *J. Chem. Inf. Model.* **2005**, *45*, 1017–1023.
- (7) Aparna, V.; Rambabu, G.; Panigrahi, S. K.; Sarma, J. A.; Desiraju, G. R. Virtual screening of 4-anilinoquinazoline analogues as EGFR kinase inhibitors: importance of hydrogen bonds in the evaluation of poses and scoring functions. *J. Chem. Inf. Model.* **2005**, *45*, 725–738.
- (8) Forino, M.; Jung, D.; Easton, J. B.; Houghton, P. J.; Pellecchia, M. Virtual docking approaches to protein kinase B inhibition. *J. Med. Chem.* **2005**, *48*, 2278–2281.
- (9) Cummings, M. D.; DesJarlais, R. L.; Gibbs, A. C.; Mohan, V.; Jaeger, E. P. Comparison of automated docking programs as virtual screening tools. *J. Med. Chem.* **2005**, *48*, 962–976.
- (10) Manning, G.; Whyte, D. B.; Martinez, R.; Hunter, T.; Sudarsanam, S. The protein kinase complement of the human genome. *Science* **2002**, *298*, 1912–1934.
- (11) Woodburn, J. R. The epidermal growth factor receptor and its inhibition in cancer therapy. *Pharmacol. Ther.* **1999**, *82*, 241–250.
- (12) Morgan, D. O. Cyclin-dependent kinases: engines, clocks, and microprocessors. *Annu. Rev. Cell Dev. Biol.* **1997**, *13*, 261–291.
- (13) Garrett, M. D.; Fattaey, A. CDK inhibition and cancer therapy. *Curr. Opin. Genet. Dev.* **1999**, *9*, 104–111.
- (14) Meijer, L.; Leclerc, S.; Leost, M. Properties and potential-applications of chemical inhibitors of cyclin-dependent kinases. *Pharmacol. Ther.* **1999**, *82*, 279–284.
- (15) Webster, K. R. The therapeutic potential of targeting the cell cycle. *Expert Opin. Invest. Drugs* **1998**, *7*, 865–887.
- (16) Chen, Y. N.; Sharma, S. K.; Ramsey, T. M.; Jiang, L.; Martin, M. S.; Baker, K.; Adams, P. D.; Bair, K. W.; Kaelin, W. G., Jr. Selective killing of transformed cells by cyclin/cyclin-dependent kinase 2 antagonists. *Proc. Natl. Acad. Sci. U.S.A.* **1999**, *96*, 4325–4329.
- (17) Pines, J. Cyclins and cyclin-dependent kinases: take your partners. *Trends Biochem. Sci.* **1993**, *18*, 195–197.
- (18) Gillett, C. E.; Barnes, D. M. Demystified ... cell cycle. *Mol. Pathol.* **1998**, *51*, 310–316.
- (19) Barvian, M.; Boschelli, D. H.; Cossrow, J.; Dobrusin, E.; Fattaey, A.; Fritsch, A.; Fry, D.; Harvey, P.; Keller, P.; Garrett, M.; La, F.; Leopold, W.; McNamara, D.; Quin, M.; Trumpp-Kallmeyer, S.; Toogood, P.; Wu, Z.; Zhang, E. Pyrido[2,3-d]pyrimidin-7-one inhibitors of cyclin-dependent kinases. *J. Med. Chem.* **2000**, *43*, 4606–4616.

- (20) Bramson, H. N.; Corona, J.; Davis, S. T.; Dickerson, S. H.; Edelstein, M.; Frye, S. V.; Gampe, R. T., Jr.; Harris, P. A.; Hassell, A.; Holmes, W. D.; Hunter, R. N.; Lackey, K. E.; Lovejoy, B.; Luzzio, M. J.; Montana, V.; Rocque, W. J.; Rusnak, D.; Shewchuk, L.; Veal, J. M.; Walker, D. H.; Kuyper, L. F. Oxindole-based inhibitors of cyclin-dependent kinase 2 (CDK2): design, synthesis, enzymatic activities, and X-ray crystallographic analysis. *J. Med. Chem.* **2001**, *44*, 4339–4358.
- (21) Gussio, R.; Zaharevitz, D. W.; McGrath, C. F.; Pattabiraman, N.; Kellogg, G. E.; Schultz, C.; Link, A.; Kunick, C.; Leost, M.; Meijer, L.; Sausville, E. A. Structure-based design modifications of the paullone molecular scaffold for cyclin-dependent kinase inhibition. *Anticancer Drug Des.* **2000**, *15*, 53–66.
- (22) Shewchuk, L.; Hassell, A.; Wisely, B.; Rocque, W.; Holmes, W.; Veal, J.; Kuyper, L. F. Binding mode of the 4-anilinoquinazoline class of protein kinase inhibitor: X-ray crystallographic studies of 4-anilinoquinazolines bound to cyclin-dependent kinase 2 and p38 kinase. *J. Med. Chem.* **2000**, *43*, 133–138.
- (23) Tang, J.; Shewchuk, L. M.; Sato, H.; Hasegawa, M.; Washio, Y.; Nishigaki, N. Anilino-pyrazole as selective CDK2 inhibitors: design, synthesis, biological evaluation, and X-ray crystallographic analysis. *Bioorg. Med. Chem. Lett.* **2003**, *13*, 2985–2988.
- (24) Rella, M.; Rushworth, C. A.; Guy, J. L.; Turner, A. J.; Langer, T.; Jackson, R. M. Structure-based pharmacophore design and virtual screening for novel Angiotensin converting enzyme 2 inhibitors. *J. Chem. Inf. Model.* **2006**, *46*, 708–716.
- (25) Brooks, B. R.; Bruccoleri, R. E.; Olafson, B. D.; States, D. J.; Swaminathan, S.; Karplus, M. CHARMM: A program for macromolecular energy, minimization, and dynamics calculations. *J. Comput. Chem.* **1983**, *4*, 187–217.
- (26) Accelrys Inc.: San Diego, CA, U.S.A.
- (27) Tripos Inc.: St. Louis, MO, U.S.A.
- (28) Bohm, H. J. The development of a simple empirical scoring function to estimate the binding constant for a protein–ligand complex of known three-dimensional structure. *J. Comput.-Aided Mol. Des.* **1994**, *8*, 243–256.
- (29) Kramer, B.; Rarey, M.; Lengauer, T. Evaluation of the FLEXX incremental construction algorithm for protein–ligand docking. *Proteins* **1999**, *37*, 228–241.
- (30) Rarey, M.; Kramer, B.; Lengauer, T.; Klebe, G. A fast flexible docking method using an incremental construction algorithm. *J. Mol. Biol.* **1996**, *261*, 470–489.
- (31) The Cambridge Crystallographic Data Centre: Cambridge, U.K.
- (32) Jones, G.; Willett, P.; Glen, R. C. A genetic algorithm for flexible molecular overlay and pharmacophore elucidation. *J. Comput.-Aided Mol. Des.* **1995**, *9*, 532–549.
- (33) Jones, G.; Willett, P.; Glen, R. C. Molecular recognition of receptor sites using a genetic algorithm with a description of desolvation. *J. Mol. Biol.* **1995**, *245*, 43–53.
- (34) Jones, G.; Willett, P.; Glen, R. C.; Leach, A. R.; Taylor, R. Development and validation of a genetic algorithm for flexible docking. *J. Mol. Biol.* **1997**, *267*, 727–748.
- (35) Venkatachalam, C. M.; Jiang, X.; Oldfield, T.; Waldman, M. Ligand-Fit: a novel method for the shape-directed rapid docking of ligands to protein active sites. *J. Mol. Graphics Modell.* **2003**, *21*, 289–307.
- (36) Gehlhaar, D. K.; Verkhivker, G. M.; Rejto, P. A.; Sherman, C. J.; Fogel, D. B.; Fogel, L. J.; Freer, S. T. Molecular recognition of the inhibitor AG-1343 by HIV-1 protease: conformationally flexible docking by evolutionary programming. *Chem. Biol.* **1995**, *2*, 317–324.
- (37) Gehlhaar, D. K.; Bouzida, D.; Rejto, P. A. *Rational Drug Design: Novel Methodology and Practical Applications*; Parrill, L., Reddy, M. R., Eds.; American Chemical Society: Washington, DC, 1999; pp 292–311.
- (38) Mayo, S. L.; Olafson, B. D.; Goddard, W. A. I. DREIDING: A generic force field. *J. Phys. Chem.* **1990**, *94*, 8897–8909.
- (39) Dinur, U.; Hagler, A. T. Direct Evaluation of Nonbonding Interactions from ab Initio Calculations. *J. Am. Chem. Soc.* **1989**, *111*, 5149–5151.
- (40) Meng, E. C.; Shoichet, B. K.; Kuntz, I. D. Automated docking with grid-based energy evaluation. *J. Comput. Chem.* **1992**, *13*, 505–524.
- (41) Weiner, S. J.; Kollman, P. A.; Nguyen, D. T.; Case, D. A. An all atom force field for simulations of proteins and nucleic acids. *J. Comput. Chem.* **2005**, *7*, 230–252.
- (42) Eldridge, M. D.; Murray, C. W.; Auton, T. R.; Paolini, G. V.; Mee, R. P. Empirical scoring functions: I. The development of a fast empirical scoring function to estimate the binding affinity of ligands in receptor complexes. *J. Comput.-Aided Mol. Des.* **1997**, *11*, 425–445.
- (43) Muegge, I.; Martin, Y. C. A general and fast scoring function for protein–ligand interactions: a simplified potential approach. *J. Med. Chem.* **1999**, *42*, 791–804.
- (44) Krammer, A.; Kirchhoff, P. D.; Jiang, X.; Venkatachalam, C. M.; Waldman, M. LigScore: a novel scoring function for predicting binding affinities. *J. Mol. Graphics Modell.* **2005**, *23*, 395–407.
- (45) Jain, A. N. Scoring noncovalent protein–ligand interactions: a continuous differentiable function tuned to compute binding affinities. *J. Comput.-Aided Mol. Des.* **1996**, *10*, 427–440.

CI600186B